Measurement of Meson Electroproduction Differential Cross Sections for η', ω, and ρ^0 (E'OR) in the Threshold Region Using HKS-HES Setup

HKS Collaboration Proposal in Hall C for PAC54

Ralph M. Marinaro III

JLab PAC54 — July 6-10, 2026

Christopher Newport University

1. Purpose of this presentation

For PAC54 members:

- Provide an overview of the E'OR experimental proposal that was submitted as a Hall C experiment using the HKS–HES apparatus.
- Address how collaborator and TAC report commentary was used as feedback for improving the success of the E'OR experiment.
- Confirm that the experimental concept is feasible as a configuration where HES measures e', HKS measures p' in coincidence, and the undetected X meson is reconstructed via missing mass.

Primary message

E'OR is an opportunistic, semi-parasitic low-Q^2 meson electroproduction experiment that uses the already planned HKS–HES infrastructure for the hyper-nuclear program to fill a largely uncovered region between photoproduction and higher-Q^2 electroproduction data, and to further increase the scientific return.

2. Physics gap in low-Q^2 exclusive meson electroproduction

- Channels: $ep \to e'p'M$, with $M = \rho^0, \omega, \eta'$, target region near threshold $Q^2 \approx 0.015$–$0.06\ \mathrm{GeV}^2$.
- Existing data are concentrated near photoproduction or at $Q^2 > 0.1\ \mathrm{GeV}^2$, E'OR helps fill the data gap.

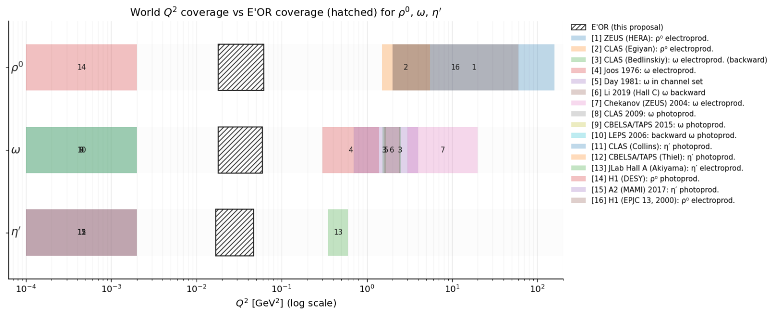

Physics motivation

Anchor the transition from $Q^2 = 0$ photoproduction to higher Q^2 electroproduction with high-resolution missing-mass reconstruction and precision differential cross sections.

3. Why low-Q^2 and near threshold?

Low-Q^2 controlled virtuality near photoproduction

- Electroproduction introduces photon virtuality as a tunable scale beyond real-photon production.
- Low-Q^2 data anchor how the reaction evolves away from $Q^2 = 0$ photoproduction.
- This region constrains the hadronic baseline before higher-Q^2 or partonic interpretations are applied.
- Unseparated Q^2 dependence constrains how combined virtual-photon response evolves from photoproduction limit.

Near threshold amplified sensitivity to reaction dynamics

- Restricted phase space tightly constrains the allowed final-state kinematics.
- Interference among competing amplitudes can produce larger effects in measured cross sections.
- t-dependence is especially sensitive to exchange mechanisms, form factors, and Regge trajectories.
- Natural/unnatural-parity exchange balance and possible resonance contributions are more exposed.

Why E'OR is positioned here

High-resolution missing-mass reconstruction in HKS–HES gives differential cross sections and t-slopes in the low-Q^2, near-threshold region where existing data are sparse and theoretical discrimination is strong.

4. Why measure ρ^0?

ρ^0 is the vector-meson reference channel

The ρ^0 channel provides control for vector-meson electroproduction, anchoring measurements where dominant mechanisms are comparatively well studied.

Benchmark reaction dynamics

- Standard descriptions include vector-meson dominance, hadronic photon coupling, t-channel exchange, and diffractive-like production.
- at forward angles, ρ^0 production is closely associated with natural-parity exchange, including Pomeron-like contributions.
- Near threshold, departures from a simple diffractive picture are more visible.

Why it makes sense for E'OR

- ρ^0 is dominantly isovector: $\rho^0 \sim (u\bar{u} - d\bar{d})/\sqrt{2}$.
- It establishes the isovector vector-meson baseline for comparison with the isoscalar ω.
- It tests whether the low-Q^2, near-threshold region follows established vector-meson systematics.
- Anchors vector-meson sector and provides reference for interpreting more selective ω and η' physics.

5. Why measure ω?

ω is the controlled isoscalar contrast to ρ^0

The ω channel asks whether the same production picture that describes the isovector ρ^0 also describes an isoscalar vector meson at the same low-Q^2, near-threshold kinematics.

Isospin and exchange sensitivity

- ω and ρ^0 are neutral vector mesons, $J^{PC} = 1^{--}$.
- The ω is dominantly isoscalar: $\omega \sim (u\bar{u} + d\bar{d})/\sqrt{2}$.
- This makes ω the clean contrast to the isovector ρ^0 benchmark.
- Comparing channels isolates isospin-dependent reaction dynamics, where ω is isoscalar and pion-exchange-sensitive contrast to ρ^0.

Near-threshold physics role

- ω production is expected to be more sensitive to pion exchange than ρ^0.
- Pion exchange is an unnatural-parity contribution, distinct from natural-parity Pomeron-like or tensor-meson exchange.
- Different ω strength or t behavior compared to ρ^0 suggests altered balance of exchange mechanisms.

6. Why measure η'?

η' extension beyond vector-mesons

The η' channel is qualitatively different from ρ^0 and ω. It probes flavor-singlet pseudoscalar dynamics tied to the axial $U(1)$ anomaly, providing a channel where E'OR can test whether conventional hadronic exchange mechanisms are sufficient.

Flavor-singlet QCD sensitivity

- The η' is not an ordinary octet pseudoscalar, tied to axial $U(1)$ anomaly and structure of gluon fields.
- Wave function contains a substantial flavor-singlet component, making it sensitive to dynamics not isolated by ρ^0 or ω.
- η' production probes singlet-sensitive couplings rather than only standard non-singlet hadronic exchange.

Near-threshold structure sensitivity

- Restricted phase space magnifies sensitivity to model assumptions in the production amplitude.
- Singlet-specific or gluonic contributions may appear as deviations from purely hadronic descriptions.
- Near $W \approx 1.91\ \mathrm{GeV}$, close to the region where η' may couple to $N(1895)\,1/2^-$, channel connects to baryon-excitation and possible hidden-strangeness.

7. Observables and channel separation

- Reaction formalism:

$$e(k) + p(p) \to e'(k') + p'(p') + X$$

- Missing mass calculation:

$$M_X^2 = (k + p - k' - p')^2$$

- Primary observables include:

$$\frac{d\sigma}{dQ^2}, \qquad \frac{d\sigma}{dt}, \qquad \sigma_\omega/\sigma_{\rho^0}, \qquad \sigma_{\eta'}/\sigma_\omega.$$

- For missing mass, mesons ω and η' have sharp peaks and ρ^0 is broader with large intrinsic decay width ($\Gamma \approx 149$ MeV)

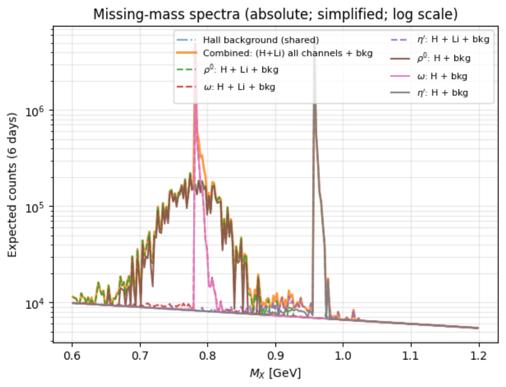

Projected missing-mass spectra including signal, Li, continuum, and hall background.

8. Beam-current after TAC target comments

TAC comment addressed:

The TAC and target-group comments noted that LiH target properties are still under development and that hydrogen dissociation under electron irradiation may require operation below the submitted 30 μA current. The simulation was therefore repeated at reduced beam current to test whether E'OR remains statistically viable.

Channel	Submitted case	Reduced-current cases	Worst-bin raw stat. uncertainty
ρ^0	30 μA, 6 d	5 or 1 μA, 6 d	0.142% $\rightarrow$ 0.35% $\rightarrow$ 0.78%
ω	30 μA, 6 d	5 or 1 μA, 6 d	0.146% $\rightarrow$ 0.36% $\rightarrow$ 0.80%
η'	30 μA, 6 d	5 or 1 μA, 6 d	0.108% $\rightarrow$ 0.26% $\rightarrow$ 0.59%

Response

Even at 1 μA, the raw statistical uncertainty remains below 1% in all channels. The measurement remains limited by controlled systematics rather than counting statistics.

9. Simulation and analysis chain made explicit

TAC comment addressed:

More explicitly state detector response, tracking/PID efficiencies, reconstruction, and beam effects in simulation.

Event generation and acceptance

- Generate $ep \to e'p'M$ with two-body $\gamma^* p \to p'M$ kinematics, HES samples scattered electrons near 8.5°, $p_{e'} \approx 0.740\ \mathrm{GeV}/c$ and HKS accepts recoil protons near 11.5° with channel-dependent central momentum, acceptance is applied in (θ, ϕ, p) using HES/HKS angular and momentum bites.

Detector and analysis response

- Track smearing applied to electron and proton momentum and angles, efficiency model includes tracking, trigger, proton PID, live-time, and analysis-cut factors, proton PID taken from TOF mass reconstruction plus Cherenkov veto response, radiative spread modeled with a one-sided scattered-electron energy-loss tail.

Extraction workflow

Events are reconstructed in missing mass, binned in Q^2, W, and $-t$, corrected for acceptance, bin-centering, efficiency, radiative effects, and Li/background subtraction, then propagated into differential cross sections.

10. Simulation clarifications for PAC readers

What was used for the submitted E'OR projections

- The proposal projections use an author-developed **fast, analysis-level Monte Carlo**, not a full GEANT4 transport simulation.
- Events are generated for $ep \to e' p' M$ using exact two-body $\gamma^* p \to p' M$ kinematics, then weighted by channel-dependent input $d\sigma/dt$ models.
- HES/HKS acceptance is applied through angular and momentum bites, reconstructed quantities include smeared Q^2, W, t, and missing mass.
- Tracking, trigger, PID, live-time, radiative, Li-subtraction, and acceptance effects are included as correction factors or parameterized response terms.

11. Simulation clarifications for PAC readers (cont'd)

Parameterized or not yet full simulation

- Spectrometer transport, detector material, target windows, secondary production, and detailed detector response are not yet modeled with a merged full GEANT4 chain.
- Reconstruction efficiencies are inputs, bin-dependent parameterizations, not full detector reconstruction.
- LiH target backgrounds are generated as separate Li and continuum components with independent slopes and Q^2 dependence, then propagated through the same missing-mass extraction.
- "hall background" means non-exclusive accidental/random coincidence and hall-rate background, modeled phenomenologically as smooth shape.

Path to final robustness

- Separate GEANT4 simulations exist for HES and HKS and are being merged as the replacement simulation for E'OR.
- The merged GEANT4 simulation will provide the final transport-based acceptance, material/target-region background estimates, and detector-response validation.
- The current fast MC remains useful for closure tests, binning studies, yield scaling, model-dependence checks, and cross-checks against the full simulation.
- Fast MC for submitted projections, during experimental development merge HKS–HES GEANT4 for final acceptance/background validation.

12. HES electron selection and pion contamination

PAC comment addressed

HES does not have a e/π PID, identifies scattered-electron through charge/optics, tracking, scintillator timing, coincidence with HKS, and exclusive missing-mass reconstruction.

How electron is selected

- HES operates as negative-particle arm, EDC drift chambers reconstruct track momentum and angle.
- ETOF1–ETOF2 scintillator provides HES charged-track trigger, event must satisfy HES–HKS coincidence timing, HKS provides recoil-proton identification using TOF and Cherenkov vetoes, HES track reconstructed under electron hypothesis

What the HKS–HES material says

- Existing HKS–HES proposals quote HES singles rates, not separate HES e^- and π^- components. PAC52 rate estimates list HES only as e', initial residual pion background as a scanned quantity:

$$\frac{B_{\pi^-}^{\mathrm{HES}}}{S_{e'}} = \left(\frac{R_{\pi^-}}{R_{e'}}\right)_{\mathrm{raw}} \frac{P(\pi^- \text{ fake} \to \text{window})}{P(e' \text{ signal} \to \text{window})}.$$

Fast-MC stress-test result

For assumed raw HES π^-/e' levels of 5–10%, the residual pion background after timing and missing-mass selection is estimated to be $\sim$ 5–10% for the broad ρ^0 window, $\sim$ 2–5% for ω, and $\sim$ 2–4% for η'.

13. Estimating LiH and target-material backgrounds

PAC question addressed

N_{Li} represents the non-hydrogen material contribution associated with the LiH target environment.

Current projection treatment

- LiH is modeled as one H center plus one Li nucleus per molecule, MC generates separate H signal, H continuum, and Li/material components, Li component is passed through the same HES–HKS acceptance, and is reconstructed in missing mass. In the extraction, the material term enters as a scaled subtraction.

Experimental estimate

- Use dedicated auxiliary target data to constrain backgrounds, Li target for LiH-composition background, empty-frame / hole-target data, random-coincidence for accidental backgrounds. Use missing-mass model data to normalize smooth material contributions in each channel, replace fast-MC material model with merged HKS–HES GEANT4 transport for final estimates.

PAC message

The submitted projections use a conservative parameterized Li/material subtraction. The final analysis will determine this contribution with dedicated target/background data and GEANT4 target-region transport.

14. Projected kinematic coverage and reconstructed spectra

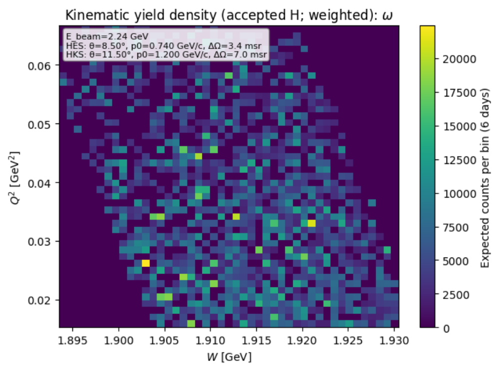

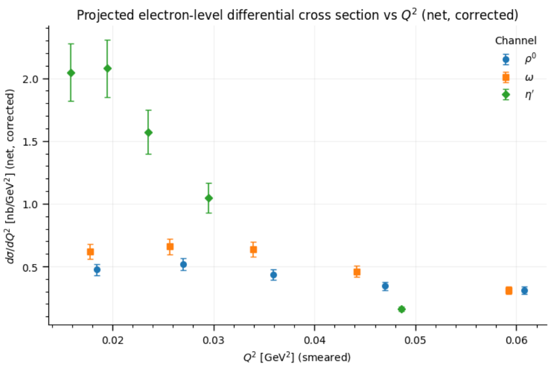

Example Q^2 vs W heat map for ω meson projected kinematic coverage.

Projected cross sections for E'OR particles, binning dependent on requested days and beam current.

15. Projected E'OR cross sections in context with CLAS data

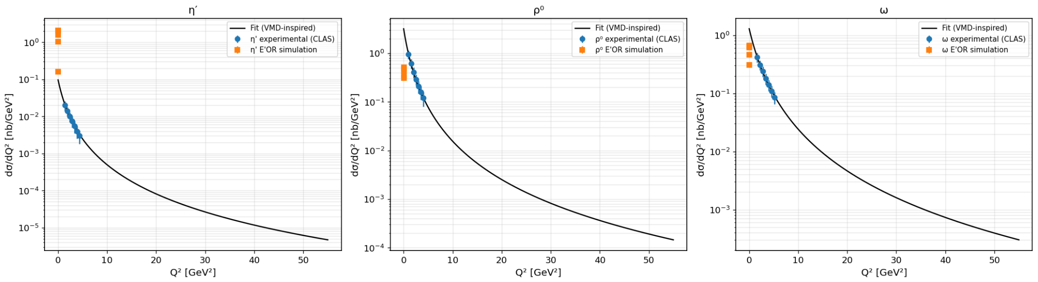

- Orange data makers are E'OR projected $d\sigma/dQ^2$ from simulation and blue are CLAS electroproduction data used as closest available benchmark.
- CLAS data are generally at higher Q^2 and somewhat different W, so the comparison is not direct.
- Projected E'OR cross sections are realistic in magnitude compared with existing electroproduction data, while adding uniquely low-Q^2 coverage for ρ^0, ω, and η'.

16. Projected t-shape model discrimination

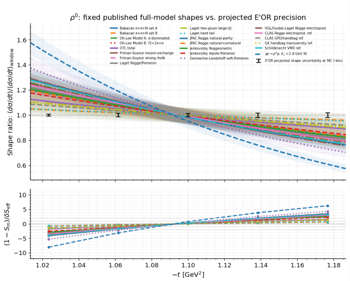

ρ^0: vector-meson benchmark

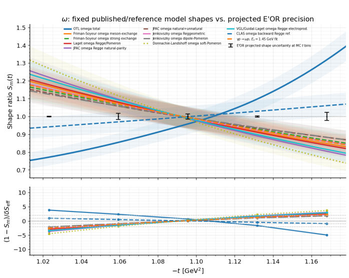

ω: isoscalar/exchange-mechanism contrast

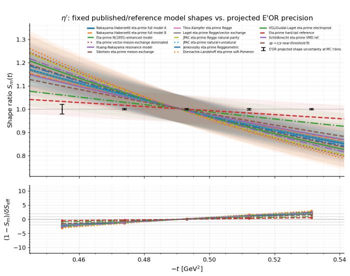

η': threshold/singlet-sensitive dynamics

How to read these plots

Colored curves are fixed external/reference model shapes normalized by each curve's own E'OR-window mean. Black points are plotted at the neutral reference $S = 1$ and show the projected bin-dependent E'OR shape uncertainty at the MC-derived $-t$ bins.

17. Revised finite-bin tables

PAC comments addressed

The proposal tables are revised (see back-up slides) so that Tables 1 and 3 no longer quote only bin centers. The experimental resolutions in $-t$ and Q^2 were evaluated from reconstructed-minus-true Monte Carlo residuals and compared directly with the analysis bin widths.

Channel / variable	Mean bin width	Mean FWHM	FWHM / width	Same-bin fraction
ρ^0, $-t$	3.83×10^{-2}	2.06×10^{-5}	5.4×10^{-4}	98.1%
ω, $-t$	3.62×10^{-2}	1.66×10^{-5}	4.6×10^{-4}	98.2%
η', $-t$	1.91×10^{-2}	2.59×10^{-6}	1.4×10^{-4}	99.7%
ρ^0, Q^2	1.09×10^{-2}	5.30×10^{-4}	4.9%	96.5%
ω, Q^2	1.09×10^{-2}	4.93×10^{-4}	4.6%	95.5%
η', Q^2	9.99×10^{-3}	4.06×10^{-4}	6.4%	90.9%

Result

The reconstructed $-t$ resolution is negligible compared with the bin width. The reconstructed Q^2 resolution is also much smaller than the analysis bins, with typical FWHM/bin-width ratios of 5–6% and same-bin containment above 90%.

18. Bin-centering convention and model dependence

PAC comment addressed

The primary E'OR result will no longer be reported as a model-centered point cross section, but as a finite-bin, bin-averaged cross section over the stated bin edges.

Primary reported quantity

$$\left\langle \frac{d\sigma}{dx} \right\rangle_{\rm bin} = \frac{1}{\Delta x} \int_{x_{\rm low}}^{x_{\rm high}} \frac{d\sigma}{dx}\, dx, \qquad x = -t,\ Q^2.$$

- Tables give explicit bin edges and widths, measurement assigned to finite bin, no bin-centering.

Bin-centering diagnostic

Channel	$\langle \lvert C_i - 1 \rvert \rangle$	$\max \lvert C_i - 1 \rvert$
ρ^0	0.22%	0.22%
ω	0.20%	0.20%
η'	0.055%	0.055%

C_i is retained only as a model-dependence diagnostic.

Result

The updated analysis avoids bin-centering model dependence in the primary reported cross sections. The old bin-centering is retained only to quantify size of effect, which is below 0.3%.

19. Why HKS–HES is the enabling apparatus

- HES selects forward-angle scattered electrons at low momentum transfer, HKS detects recoil hadron, for E'OR this is used as a proton arm rather than a kaon arm.
- High-resolution magnetic spectrometer is essential for clean missing-mass reconstruction.
- E'OR requires no new detector resources and uses existing HKS–HES installation plan.
- Projected DAQ performance lowers concerns to suppress scattered protons at the online trigger level, separate kaon-proton trigger possible.

Strategic motivation

E'OR is an opportunistic high-resolution experiment enabled by a configuration that is already approved for the Hall C HKS program.

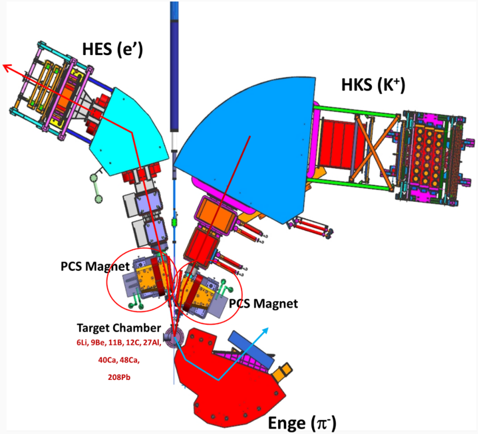

HKS–HES layout planned for hypernuclear program in JLab Hall C.

20. Baseline kinematics and run conditions

Quantity	Beam / target	HES	HKS
Beam energy	2.24 GeV	–	–
Current	~~30 μA~~	–	–
Target	LiH, 150 mg/cm^2	–	–
Central angle	–	8.5°	11.5°
Central momentum	–	0.740 GeV/c	channel dependent
Solid angle	–	3.4 msr	7.0 msr
Momentum bite	–	$\pm4\%$	$\pm6\%$

ρ^0 and ω setting

$p_{0,\mathrm{HKS}} \approx 1.20$ GeV/c, measured simultaneously.

η' setting

$p_{0,\mathrm{HKS}} \approx 0.75$ GeV/c, scale HKS magnet by $\sim 60\%$.

21. LiH target development plan and beam current

PAC concern addressed

E'OR uses LiH target at $150\,\mathrm{mg/cm^2}$ and ~~30 μA~~, the target effort is still in design and validation.

Target-development status

- Part of solid-target system for HKS program.
- Design includes scattering chamber, cold ladder, cryogenic interface, motion system, instrumentation, interlocks, and a proposed load-lock for oxygen-sensitive targets.
- LiH requires controlled handling, load-lock/cartridge limits exposure during installation and target changes.
- Ongoing target studies include thermal analysis, raster requirements, ladder design, motion/alignment.

E'OR operating plan

- E'OR current set by target qualifications, allowable temperature, hydrogen retention, raster stability, and target inspection.
- Reduced-current studies at 5 and 1 μA show the measurement remains statistically viable, the dominant limitation remains systematic control.
- Before production running, E'OR requires a target checkout sequence: low-current beam test, raster scan, temperature/interlock validation, yield-stability check, and current ramp only if target response is stable.

22. Beam-parameter requirements relative to approved HKS–HES

PAC question addressed

E'OR does not require beam conditions more stringent than the approved HKS–HES hypernuclear program.

Parameter	Approved HKS–HES campaign	E'OR requirement
Beam energy	2.24 GeV one-pass beam.	Same 2.24 GeV beam energy.
Beam-energy spread	The hypernuclear missing-mass spectroscopy requires high beam stability, typically $\Delta E/E \lesssim 10^{-4}$ FWHM.	No need for tighter beam control than hypernuclear spectroscopy.
Beam current	Some HKS–HES solid-target settings use 50 μA.	Submitted case was ~~30 μA~~,t 5 and 1 μA remain statistically viable.
Spectrometer settings	Standard HKS–HES setting: HES near 0.740 GeV/c, HKS near 1.20 GeV/c.	$\rho^0+\omega$ use the same, η' setting lowers HKS to $\sim$ 0.75 GeV/c, requires optics validation, not stricter beam parameters.
Raster, target limits	Target-dependent raster and current limits are part of HKS operation.	Final E'OR current and raster will follow LiH target qualifications.

23. Beam spot, raster, and stray-field

TAC concern addressed

Specify beam-position, raster, and optics requirements, E'OR will use HKS-HES beamline readiness plan with additional TOSCA/beam-tracking check for lower-HKS η' setting.

Beam spot and raster requirements

- Target ~ 6.6 m downstream of Hall-C pivot. E'OR will use HKS beamline BPM/harp monitoring plan and explicit LiH raster, with nominal starting point $2 \times 2\ \mathrm{mm}^2$. Final raster and current set by LiH target thermal qualification, temperature, hydrogen retention, current and yield stability.

HKS setting and stray-field validation

- $\rho^0 + \omega$ use HKS $p_0 \approx 1.20$ GeV/c, η' uses $p_0 \approx 0.75$ GeV/c, so beamline optics and stray-field must be recalculated. TOSCA field-map update in development for beamline studies. E'OR readiness task is rerun TOSCA/beam-tracking at lower HKS momentum and find required beamline parameters.

Readiness path

Validation checklist for magnetic settings includes, primary beam reaches dump with acceptable orbit, no aperture-loss issue near target/PCS/HKS/HES, corrector/shielding settings defined, MPS/FSD thresholds updated for lower HKS magnet current.

24. Beamtime request submitted to PAC54

Setting	E_b	I	Target	Beamtime
$\rho^0 + \omega$, HKS $p_0 \approx 1.20\,\mathrm{GeV/c}$	$2.24\,\mathrm{GeV}$	~~$30\ \mu$A~~	LiH	6.0 d
η', HKS $p_0 \approx 0.75\,\mathrm{GeV/c}$	$2.24\,\mathrm{GeV}$	~~$30\ \mu$A~~	LiH	6.0 d
HKS momentum retuning	–	–	–	0.5 d
Elastic/optics/timing calibration	–	–	–	0.5 d
Total				**13 d**

- The spectrometer angles stay fixed, only the HKS field setting changes between the two production periods.
- Overlap with hypernuclear program $\Lambda - \Sigma$ calibrations may reduce the effective E'OR-specific overhead.
- Beamtime request is stated as beam-on-target time at 100% availability.

25. Statistics versus run length at 1 μA

PAC comment addressed

Projected uncertainties are dominated by target, acceptance, and background-subtraction systematics, the statistical precision was scanned versus production time at the conservative 1 μA current.

Channel	1 d	2 d	3 d	4 d	6 d	Dominant limit
ρ^0	1.91%	1.35%	1.10%	0.96%	0.78%	systematics
ω	1.96%	1.39%	1.13%	0.98%	0.80%	systematics
η'	1.45%	1.02%	0.83%	0.72%	0.59%	systematics

Entries are worst-bin raw statistical uncertainties at 1 μA.

Result

Worst-bin statistical uncertainty at the $\sim$ 1–2% level. Submitted 6-day-per-setting request was not driven by counting statistics alone, but to provide margin for target stability, beam consistency, and channel-by-channel cross-checks. Can decrease to fewer days following PAC guidance.

26. Systematic uncertainty inventory I: normalization, target, beam

Individual uncertainty source	**Expected range**	**How constrained / comment**
Beam charge integration	1–2%	BCM calibration, accumulated-charge scaler comparison.
BCM pedestal / current-offset stability	0.5–1%	Beam-off and low-current pedestal checks.
Beam-current stability during run	0.5–1%	Run-by-run charge-normalized yield stability.
DAQ live-time correction	0.5–1.5%	CODA live-time scalers, trigger-rate dependence.
Trigger prescale / trigger bookkeeping	$< 0.5\%$	Prescale accounting and trigger-supervisor scalers.
LiH areal density	2–3%	Target metrology and mass/thickness survey.
LiH stoichiometry / H:Li composition	1–3%	Material assay and controlled handling history.
LiH thickness uniformity	1–2%	Raster-position dependence and target survey.
Hydrogen retention under beam	2–4%	Yield-stability before and after beam exposure.
Beam heating / target-temperature dependence	1–3%	Temperature sensors, current-ramp, and yield drift.
Raster-size calibration	0.5–1.5%	Raster-current readback and harp/BPM checks.
Raster centering on target	0.5–1.5%	BPM/harp centering and target-yield stability.
Target ladder positioning	0.5–1%	Survey, encoder readback, and optics/elastic checks.
Target-frame / support material normalization	1–3%	Empty-frame, hole-target, or matched dummy target data.
Dominant items in this group	–	LiH density/composition, hydrogen retention, and target-temperature/raster stability.

27. Systematic uncertainty inventory II: spectrometers and PID

Individual uncertainty source	**Expected range**	**How constrained / comment**
HES geometric aperture acceptance	1–2%	Elastic/optics data and acceptance-edge studies.
HKS geometric aperture acceptance	1–3%	Optics, sieve/slit studies, acceptance-edge scans.
HES optics matrix / transport reconstruction	1–2%	Optics calibration, reconstructed elastic kinematics.
HKS optics matrix / transport reconstruction	1–3%	HKS optics calibration and missing-mass closure.
Lower-field HKS η' optics setting	2–4%	Dedicated optics validation at $p_0 \approx 0.75\ \mathrm{GeV}/c$.
HES central momentum calibration	0.5–1%	Elastic peak and beam-energy constraint.
HKS central momentum calibration	0.5–1%	Missing-mass calibration, elastic/proton calibration.
Spectrometer angle / pointing calibration	0.5–1%	Survey and elastic kinematic closure.
Vertex reconstruction / target-position dependence	0.5–1.5%	Vertex cuts and target-ladder position scans.
HES tracking efficiency	1–2%	Redundant tracking and track-quality variation.
HKS tracking efficiency	1–2%	Redundant tracking and track-quality variation.
HES detector-plane efficiency	0.5–1.5%	Plane-by-plane efficiency from data.
HKS detector-plane efficiency	0.5–1.5%	Plane-by-plane efficiency from data.
Coincidence-trigger efficiency, prescale	0.5–1.5%	Replay, redundancy, prescale accounting, TS scalers.
Coincidence timing cut	0.5–1.5%	Timing-window variation and sideband tests.
Proton TOF PID cut	1–2%	PID-cut variation and clean proton control samples.
Cherenkov veto efficiency / contamination	1–2%	Veto efficiency calibration and cut variation.
Electron-arm particle selection	0.5–1%	HES track/trigger quality and electron-arm stability.
Dominant items from this group	–	HKS geometric acceptance, HKS optics, and lower-field η' optics validation.

28. Systematic uncertainty inventory III: extraction and backgrounds

Individual uncertainty source	Expected range	How constrained / comment
Random-coincidence subtraction	0.5–1%	Prompt/random sidebands.
Missing-mass absolute scale	0.5–1%	Known mass peaks and calibration closure.
Missing-mass resolution model	1–2%	Peak-width comparison between data and simulation.
ρ^0 line-shape model	2–4%	Dominant for broad ρ^0 extraction; varied fit models.
ω peak template model	1–2%	Fit-range and resolution-template variation.
η' peak template model	1–2%	Fit-range and resolution-template variation.
H continuum subtraction	1–3%	Sidebands and fit-shape variation.
LiH Li-component subtraction scale k_{Li}	2–5% on yield effect	Li/dummy target, missing-mass sidebands.
Window/support subtraction scale k_{win}	1–3% on yield effect	Empty-frame/hole-target, GEANT4 material model.
Smooth hall-background template	1–2%	Randoms, sidebands, and beam-off comparisons.
Radiative correction model	1–3%	Radiative-tail variation and model comparison.
Finite-bin averaging convention	$< 0.5\%$	Finite-bin average; no bin-centering.
Bin-centering diagnostic C_i	$< 0.3\%$	Diagnostic only, not applied to primary result.
Bin migration / resolution smearing	$< 1\%$	Reco-minus-truth MC residuals, migration matrices.
Acceptance MC statistics	0.5–1%	Increase MC statistics and propagate bin-by-bin.
Input-model dependence of acceptance weighting	1–2%	Reweight events with alternate external shapes.
Dominant items from this group	–	ρ^0 line-shape extraction, Li/material subtraction, input-model dependence of acceptance weighting.

29. What optics modeling and signal extraction mean

PAC comments addressed

The revised uncertainty budget separates these into explicit sources and treats the broad ρ^0 extraction differently from the narrow ω and η' peaks.

What is included in optics modeling

- HES and HKS geometric aperture definition, transport matrices and reconstruction optics, central momentum calibration for each arm, spectrometer angle and pointing calibration, vertex dependence across the LiH target and raster area, acceptance-edge sensitivity and cut stability, magnetic-field map and ray-tracing consistency, lower-field HKS optics validation for η'.

Signal-extraction uncertainty

Channel	Peak/shape issue	Extraction syst.
ρ^0	broad line shape	2–4%
ω	narrow peak	1–2%
η'	narrow peak	1–2%

- ρ^0 has largest uncertainty because intrinsic width is large and extracted from broad missing-mass.

30. Run Plan, Collaboration Needs, and Next Steps

Run plan (baseline, submitted)

- 6 days: $\rho^0 + \omega$ @ HKS $p_0 \approx 1.20\,\text{GeV}/c$
- 6 days: η' @ HKS $p_0 \approx 0.75\,\text{GeV}/c$
- 1 day total: momentum retuning, adjust magnets, system calibrations

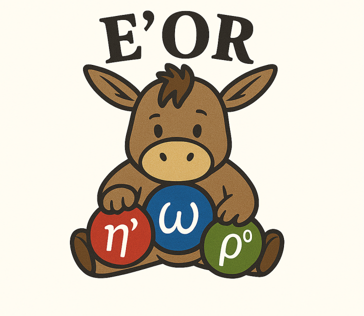

Future experiment needs

- Contingency plans, and HKS magnet adjustment procedure
- Implement proton trigger and proton PID using Cherenkov + TOF
- Improve analysis and simulation software, integrate with HKS infrastructure
- Agree on schedule and consider student theses (one per reaction channel?)

Back-up Slide: Revised proposal bin reporting (Table 1)

Table 1: Updated projected $-t$ bins.

Ch.	**Bin**	$-t_{\mathrm{low}}$	$-t_{\mathrm{cen}}$ [GeV^2]	$-t_{\mathrm{high}}$	$\Delta(-t)$	**Net yield**	**Rel. stat.**
ρ^0	1	1.00412	1.02328	1.04245	0.03833	$1.26 \times 10^6 \pm 1.12 \times 10^3$	0.089%
ρ^0	2	1.04245	1.06162	1.08078	0.03833	$1.02 \times 10^6 \pm 1.01 \times 10^3$	0.099%
ρ^0	3	1.08078	1.09995	1.11911	0.03833	$8.27 \times 10^5 \pm 9.10 \times 10^2$	0.110%
ρ^0	4	1.11911	1.13828	1.15744	0.03833	$6.19 \times 10^5 \pm 7.87 \times 10^2$	0.127%
ρ^0	5	1.15744	1.17661	1.19577	0.03833	$4.96 \times 10^5 \pm 7.04 \times 10^2$	0.142%
ω	1	1.00501	1.02312	1.04123	0.03622	$1.45 \times 10^6 \pm 1.20 \times 10^3$	0.083%
ω	2	1.04123	1.05934	1.07745	0.03622	$1.45 \times 10^6 \pm 1.20 \times 10^3$	0.083%
ω	3	1.07745	1.09557	1.11368	0.03622	$1.16 \times 10^6 \pm 1.08 \times 10^3$	0.093%
ω	4	1.11368	1.13179	1.14990	0.03622	$8.09 \times 10^5 \pm 9.00 \times 10^2$	0.111%
ω	5	1.14990	1.16801	1.18613	0.03622	$4.70 \times 10^5 \pm 6.85 \times 10^2$	0.146%
η'	1	0.44524	0.45481	0.46438	0.01914	$1.71 \times 10^6 \pm 1.31 \times 10^3$	0.077%
η'	2	0.46438	0.47394	0.48351	0.01914	$1.22 \times 10^6 \pm 1.11 \times 10^3$	0.090%
η'	3	0.48351	0.49308	0.50265	0.01914	$1.14 \times 10^6 \pm 1.07 \times 10^3$	0.094%
η'	4	0.50265	0.51222	0.52179	0.01914	$9.45 \times 10^5 \pm 9.72 \times 10^2$	0.103%
η'	5	0.52179	0.53136	0.54092	0.01914	$8.51 \times 10^5 \pm 9.23 \times 10^2$	0.108%

Back-up Slide: Revised proposal bin reporting (Table 3)

Table 2: Updated projected differential cross sections in Q^2 bins.

Ch.	**Bin**	Q^2_{low}	Q^2_{cen} [GeV^2]	Q^2_{high}	ΔQ^2	$d\sigma/dQ^2$ [nb/GeV^2]	δ
ρ^0	1	0.01397	0.01848	0.02300	0.00903	0.47483	0.04475
ρ^0	2	0.02300	0.02702	0.03105	0.00805	0.51649	0.04872
ρ^0	3	0.03105	0.03594	0.04082	0.00978	0.43638	0.04128
ρ^0	4	0.04082	0.04696	0.05310	0.01228	0.34384	0.03266
ρ^0	5	0.05310	0.06075	0.06840	0.01530	0.31224	0.02948
ω	1	0.01390	0.01781	0.02172	0.00783	0.61881	0.05805
ω	2	0.02172	0.02566	0.02959	0.00787	0.65846	0.06177
ω	3	0.02959	0.03394	0.03828	0.00868	0.63403	0.05948
ω	4	0.03828	0.04417	0.05006	0.01178	0.46041	0.04319
ω	5	0.05006	0.05927	0.06848	0.01842	0.30874	0.02897
η'	1	0.01401	0.01587	0.01773	0.00372	2.04784	0.22713
η'	2	0.01773	0.01950	0.02127	0.00354	2.07864	0.23054
η'	3	0.02127	0.02355	0.02583	0.00456	1.57221	0.17437
η'	4	0.02583	0.02951	0.03318	0.00735	1.04700	0.11613
η'	5	0.03318	0.04858	0.06397	0.03079	0.16027	0.01779